International Journal of Environmental Impacts
Vol. 7, No. 3, September, 2024, pp. 505-514
Journal homepage: http://iieta.org/journals/ijei

Cloud Computing Application for the Analysis of Land Use and Land Cover Changes in Dry Forests of Peru

Elgar Barboza[1,2*], Wilian Salazar[3], David Gálvez-Paucar[4], Lamberto Valqui-Valqui[1], Leandro Valqui[1], Luis H. Zagaceta[1], Jhony Gonzales[4], Héctor V. Vásquez[1], Carlos I. Arbizu[5]

[1] Agrostology Laboratory, Research Institute for Livestock and Biotechnology, National University Toribio Rodríguez de Mendoza de Amazonas (UNTRM), Chachapoyas 01001, Peru
[2] Professional School of Environmental Engineering and Natural Resources, Faculty of Engineering, University Technological of the Andes (UTEA), Abancay 03001, Peru
[3] Vista Florida Agricultural Experiment Station, National Institute of Agricultural Innovation (INIA), Chiclayo 14300, Peru
[4] Research Institute for Sustainable Development and Climate Change, National University of Frontera (UNF), Sullana 20103, Peru
[5] Faculty of Engineering and Agricultural Sciences, National University Toribio Rodríguez de Mendoza de Amazonas (UNTRM), Chachapoyas 01001, Peru

Corresponding Author Email: ebarboza@indes-ces.edu.pe

https://doi.org/10.18280/ijei.070312

Received: 27 July 2024
Revised: 15 September 2024
Accepted: 22 September 2024
Available online: 30 September 2024

Keywords:
Remote Sensing (RS), biodiversity, Random Forest (RF), forest monitoring, Google Earth Engine (GEE)

ABSTRACT

Dry forests are ecosystems of great importance worldwide, but in recent decades they have been affected by climate change and changes in land use. In this study, we evaluated land use and land cover changes (LULC) in dry forests in Peru between 2017 and 2021 using Sentinel-2 images, and cloud processing with Machine Learning (ML) models. The results reported a mapping with accuracies above 85% with an increase in bare soil, urban areas and open dry forest, and reduction in the area of crops and dense dry forest. Protected natural areas lost 2.47% of their conserved surface area and the areas with the greatest degree of land use impact are located in the center and north of the study area. The study provides information that can help in the management of dry forests in northern Peru.

1. INTRODUCTION

Dry forests cover 20% of the Earth's surface, which in turn account for 30% of global productivity [1, 2] They are responsible for capturing atmospheric carbon (CO_2) from biomass and soil, in addition to harboring biodiversity [3, 4], as well as helping to maintain the hydrological cycle and soil conservation [5-7]. They enable climate regulation, conservation of flora and fauna species, and provide raw materials for construction, food and medicines [8, 9]. However, in recent years, forest ecosystems are being impacted by increasing or decreasing temperature and precipitation, changes in land use and forest degradation [10]. These disturbances are often induced by the population settled in this ecosystem, which makes it vulnerable to droughts and fires with a severe biomass reduction process [11].

In the last 60 years (1960-2019), 32% of vegetation cover has been lost due to LULC changes [12], modifying the structure, functionality of forests and loss of biodiversity habitats [9]. It also increases greenhouse gas (GHG) emissions [13]. LULC changes are the main cause of forest fragmentation for the installation of crop plots, pastures and urban growth [14]. It also affects freshwater availability and conservation of natural resources [15]. Loss of soil fertility, water pollution and droughts are related to forest degradation [16]. Therefore, the analysis of forest loss should focus on its socioeconomic uses and landscape dynamics [17, 18].

Analysis of LULC changes has been used as an important tool in the multitemporal analysis of ecosystems, the implementation of policies and strategies for sustainable development [19, 20]. RS allows detecting and spatially analyzing the Spatio-temporal dynamics of LULC using different sensors and techniques [21-24]. Time series of Landsat and Sentinel-2 (S2) images have been used to identify LULC types [24-27]. Similarly, ML models and cloud computing have been applied to analyze LULC changes and map forests accurately and in near real-time [25]. Other studies applied supervised classification by applying RF due to its robustness and overcoming data noise overfitting [28], and it has been widely used in GEE [29-31]. RF has been applied in processing large volumes of data, outperforming other methods in accuracy, such as single-layer neural networks, decision trees and maximum likelihood [29, 32].

In Peru, we find the dry forest ecosystem with biological and cultural richness, scenic beauty and high endemic value [33]. In recent decades, it has experienced biodiversity loss processes due to anthropogenic activities (extractive forestry activities, agriculture and urban expansion) and climatic conditions such as high temperatures, extreme dryness, irregular occurrence of heavy rainfall and the presence of the El Niño-Southern Oscillation (ENSO) [33, 34]. Although previous works mapped the current use in the dry forest, however, the availability of methodologies and cartography is limited for this study area, which could hinder the temporal analysis of this ecosystem [35, 36]. Likewise, there is no information available related to the impacts of LULC changes in natural protected areas. Therefore, in this study we analyze the dynamics of LULC using S2 data and cloud processing throughout the Peruvian dry forest ecosystem. This will provide baseline information on areas with higher dynamics or forest loss that will be potential areas for the development of ecological recovery and restoration projects.

2. METHODS

2.1 Study area

The dry forests of Peru [37], extend along the northern coastal zone, through the departments of La Libertad, Ancash, Lambayeque, Piura, Tumbes and Cajamarca, covering a coastal strip of between 100 to 150 km, with an altitude of up to 1000 m a.s.l. [35]. This forest covers 3.6 Mha, which represents 4.7% of the total forest in Peru [38]. It is characterized by an annual rainfall of 30 to 300 mm between December and March and a mean annual temperature of 23 °C (Figure 1).

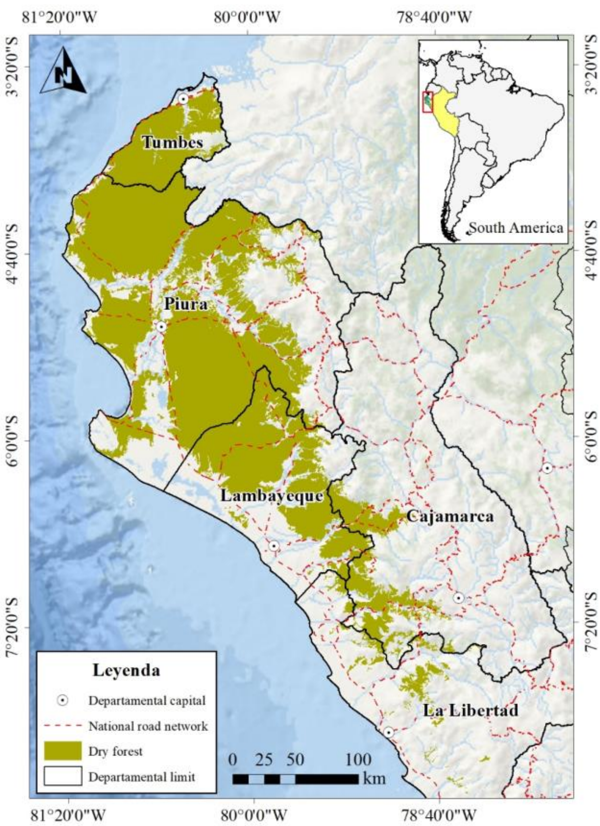

Figure 1. Forest distribution in northern Peru

The vegetation cover is characterized by being heterogeneous, with trees, shrubs and grasslands that are part of the dry forest [35]. This ecosystem harbors a diversity of forest species with canopy heights of up to 12 meters, which allows the vegetative growth of shrubs and trees [39]. Among the species that inhabit this ecosystem, it is possible to find carob *Neltuma pallida, Neltuma limensis, Vachellia macracantha, Vachellia aroma, Colicodendron scabridum, Anonna spp. and Inga spp* [40]. In addition, the dry forest of Peru also harbors animal species such as *Lycalopex sechurae, Furnarius cinnamomeus, Mazama americana, Iguana delicatissima, Tremarctos ornatus and Penelope albipennis* [38]. In the study area, land use is conditioned by anthropogenic activities (agriculture, livestock and urban growth) [24]. While vegetation depends on rainfall during the year [41].

Dry forests are of great economic importance as they provide ecosystem services such as fruits, firewood and fertilizers to the communities settled within the ecosystem. Dry forests are also used for subsistence agriculture and livestock raising, contributing to the food security of these communities. These ecosystems also host important archeological and cultural sites for tourism that help diversify local sources of income and promote the conservation of these natural and cultural environments.

Figure 2 shows process to evaluate the LULC change and its impact on the dry forest of Peru. The construction of time series of S2 images was carried out, then the extraction of clouds and cloud shadows was applied. We then compute the spectral indices and perform the RF classification using training data. Finally, the precision of the generated cartography was calculated.

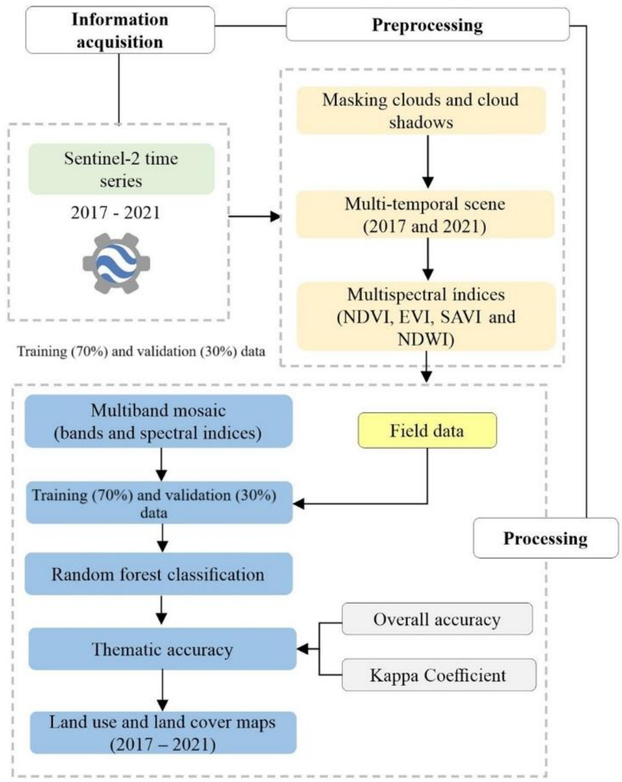

Figure 2. Evaluating LULC changes

2.2 Data collection

During the second and third week of June 2022, field trips were conducted to collect data (training and validation) in the dry forest. A GPS navigator (Garmin GPSMAP 64s) and the FocusMap application (https://www.locusmap.app/) were used to georeferenced the LULC classes and generate photographic records [42]. The LULC classes, were represented by a) Open dry forest (ODF), b) Dense dry forest (DDF), c) Bare land (BL), d) Agricultural land (AL), e) Urban area (UA) and f) Water body (WB) (Figure 3). Twenty thousand pixels were extracted from the field-collected data, representing the six randomly grouped LULC classes [24].

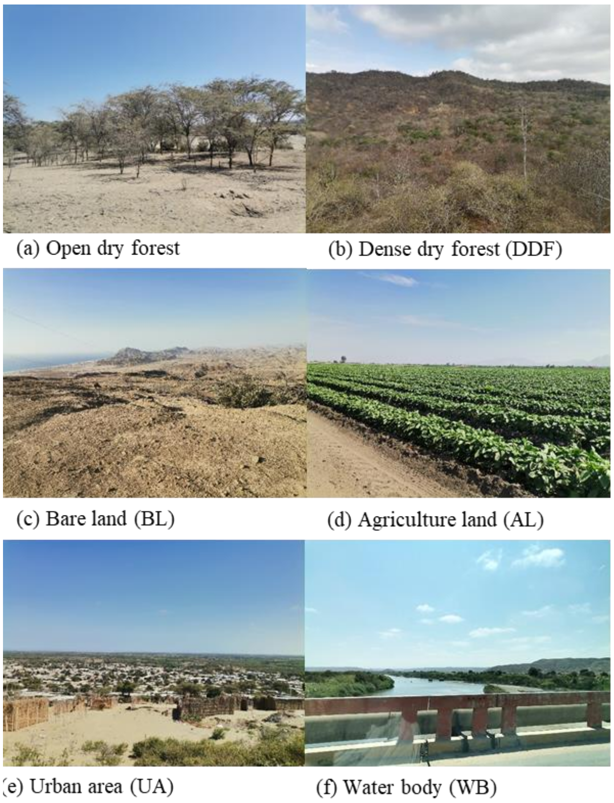

Figure 3. LULC classes in dry forests

2.3 Image processing

S2 L1C (COPERNICUS/S2) images were used due to their spatial (10 meters) and temporal (6 days) resolution. Images of a year considered <30% cloud and no cloud shadow for 2017 and 2021 [43] were selected by using the quality band (QA60). Soil-adjusted Vegetation Index (SAVI), Enhanced Vegetation Index (EVI), Normalized difference Vegetation Index (NDVI), and Normalized Difference Water Index (NDWI) were included to increase the predictor variables for LULC classification. Image processing was performed from the GEE platform [44].

The RF model was used due to its high performance to calculate a set of time series to analyses the time series [28, 45]. The RF has been applied in several studies [28, 46] and has proven to be an excellent classifier in coastal areas [47]. For this purpose, we created multiband image mosaics that included the spectral bands and indices for classification in GEE [48]. The classification results were exported and visually analyzed with high-resolution images in order to improve the classified maps of 2017 and 2021.

2.4 Validation

The precision was determined based on the confusion (error) matrix technique [49] and 456 validation points that were obtained through the formula established by Cochran [50]. These RS techniques have been widely used [51]. Similarly, we calculated (i) the overall accuracy (OA), (ii) the user's accuracy (UA), (iii) the producer's accuracy (PA) and (iv) the Kappa index was used [42, 51, 52]. Additionally, for each class and year 2017 and 2021, the intensity of changes was determined [18]. The loss or gain of each class was determined using cross-tabulation matrices [42, 53]. The annual exchange rate for FAO was calculated using Eq. (1) [54].

$$s = \left(\frac{S_2}{S_1}\right)^{1/t_2-t_1} - 1 \quad (1)$$

2.5 Land use degree index

This index quantitatively assesses the impact of human actions based on the degree of land use [55]. It is calculated according to the change in LULC compared to the natural state (Eq. (2)) [56]. The higher the degree of land use, the greater the anthropogenic transformation without taking into account the ecological environment [56].

$$l_a = 100 \times \sum_{i=1}^{n} A_i \times C_i \quad (2)$$

where, l_a is land use degree index; A_i is the rating index of the degree of land use; and C_i is the percentage of the qualified area of the i-th land use grade type. In accordance with key studies [56], LULC classes are classified according to Table 1.

Table 1. Graduated value of land use classes

LULC Class	Bare Land	Forest, Grassland and Body of Water	Agriculture Land	Urban Area
Classification Index	1	2	3	4

3. RESULTS

3.1 Land use and land cover in dry forest

The LULC of the dry forest for 2017 and 2021 is shown in Figures 4 and 5. The DDF and ODF covers are the main classes of LULC and representing 39% and 41% of DDF and 22% in ODF in 2017 and 2021, respectively and is distributed mainly in the higher altitude areas. The land area of BL has increased from 29% in 2017 to 31% in 2021 and is distributed in the desert areas of Sechura, Piura and Talara. The proportion of area of the AL class reports a reduction of area from 9% to 6% from 2017 to 2021. The AU class shows an increase, varying from 0.05 to 0.09% in 2017 and 2021, respectively. In turn, the general change of the WB was relatively small and is mainly represented by the surface of rivers located in the study area.
Overall, ODF and BL classes increased significantly, on the other hand, the cultivation area decreased, while the other LULC classes remained unchanged, such as DDF, UA and WB between 2017 and 2021.

3.2 Intensity of changes

The quantitative and spatial changes of the LULC classes were calculated in cross-tabulation matrices, which allowed showing the transformation between the different LULC classes in the dry forest for 2017 and 2021 (Table A1). From a LULC class change intensity perspective, the AU showed an increase in construction area by 2021, which came primarily from BL and ODF land. The BL acreage for 2021 changed to the establishment of new agricultural parcels and new areas of open forest cover. In turn, forest cover (DDF and ODF) showed changes due to the establishment of new agricultural plots, urban areas and soils with little vegetation. In addition, the interaction between both classes DDF and ODF. On the contrary, the area of AL showed a downward trend. Cultivated land changed to BL, ODF and DDF. At a general level between 2017 and 2021, the study area showed changing dynamics. Forest cover, BL and AU gradually increased and AL and WB classes decreased.

The loss of coverage in the dry forest in the evaluation period is mainly concentrated in areas close to urban areas and bodies of water. Between 2017 and 2021, 852.89 km^2 (2.34%) of forest cover were lost, which changed to crops, urban areas and soils with or without vegetation. Regeneration of forest cover was also reported in approximately 2,273.74 km^2 (6.24%) (Figure 6a and Table A2). At the level of protected areas (PA), 4,494.81 km^2 have been conserved so far in the entire dry forest for the regions of Cajamarca, Lambayeque, Tumbes, La Libertad and Piura. However, 110.83 km^2 (2.47%) lost forest cover (Figure 6b and Table 2).

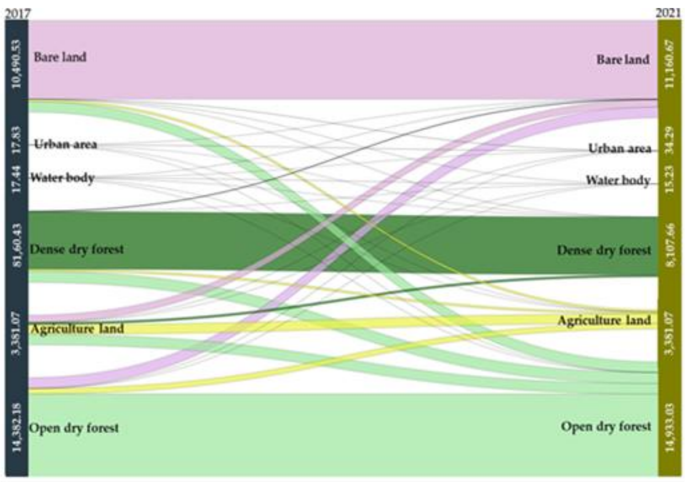

(a) Estimated areas

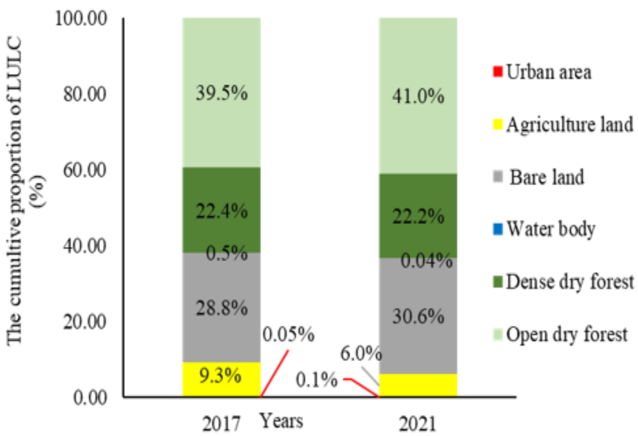

(b) Estimated proportion of each class

Figure 4. LULC area for 2017 and 2021 in the dry forest

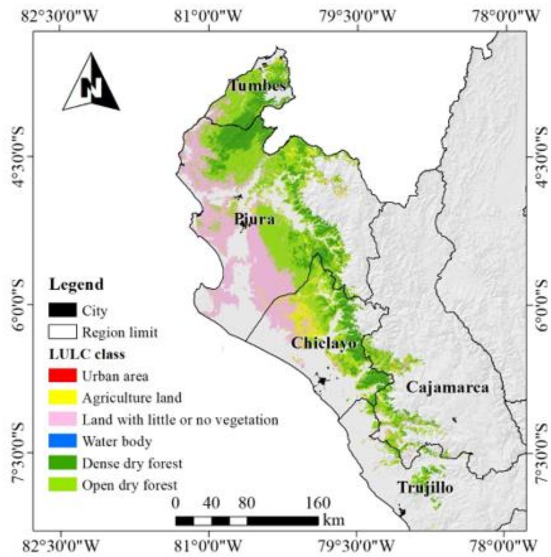

(a) 2017

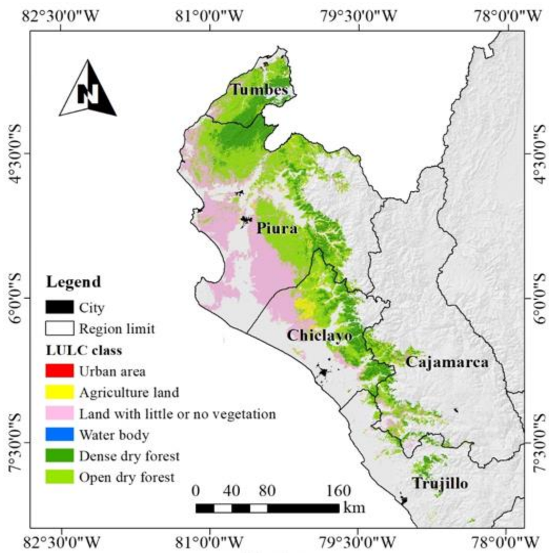

(b) 2021

Figure 5. LULC in dry forests

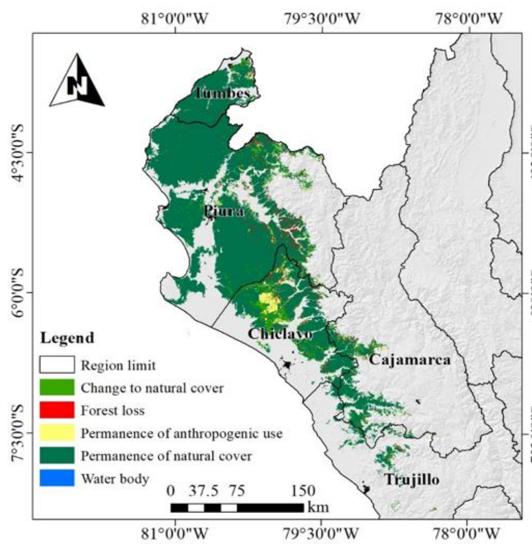

(a) LULC class transfer map in the study area

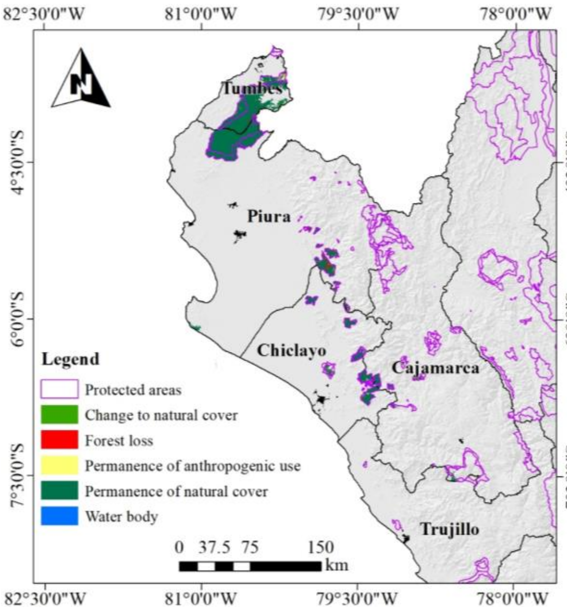

(b) LULC class transfer map in protected natural areas

Figure 6. Maps of change and persistence of LULC in the dry forest

Table 2. Area (km^2) of change and permanence of LULC

Change and permanence of the LULC	Dry Forest		Protected Areas (PA)	
	Area (km^2)	%	Area (km^2)	%
Change to natural cover	2,273.74	6.24	135.69	3.02
Forest loss	852.89	2.34	110.83	2.47
Permanence of anthropogenic use	1,385.37	3.80	76.57	1.70
Permanence of natural cover	31,922.25	87.58	4,170.39	92.78
Water body	15.23	0.04	1.34	0.03
Total	**36,449.48**	**100.00**	**4,494.81**	**100.00**

3.3 Change of degree of land use

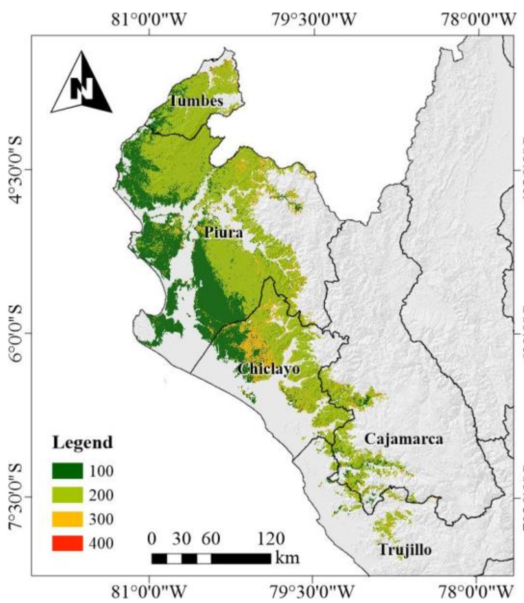

(a) 2017

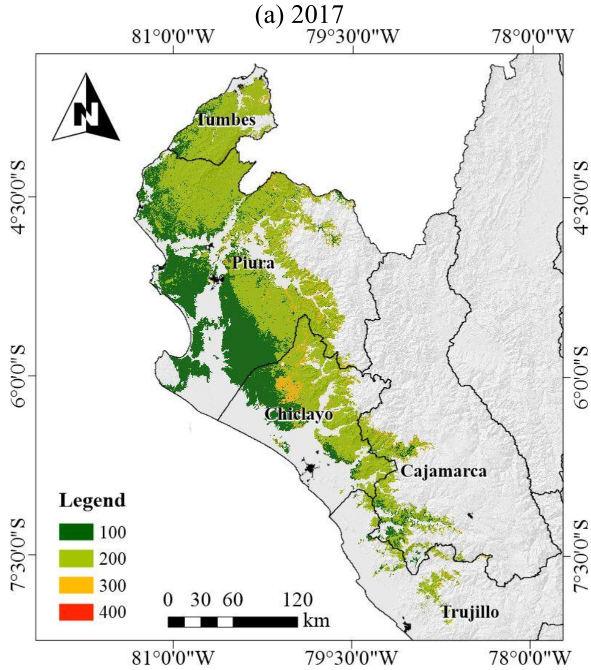

(b) 2021

Figure 7. Degree of land use for in the dry forest

The effect of human activities on the soil is reflected in the levels of use [57]. The different LULC classes identified in this analysis allowed the calculation of the comprehensive index of the degree of land use for 2017 and 2021. The range in the area varies from 100 to 200 in a similar way in both years, indicating that the areas with the highest land use are concentrated in the north of the study region, with agricultural areas predominating (Figure 7).

4. DISCUSSION

In this study, we analyze LULC changes in 2017 and 2021 using cloud computing and RF algorithm. The information generated contributes greatly to generate LULC maps for an important ecosystem in Peru, obtaining OA and Kappa accuracies greater than 89 and 85%, respectively (Table A3 and S3), indicating reasonable and reliable classification results [58]. The dynamics of LULC in the period of analysis reported an increase in the areas of bare land and the dynamics of open and dense dry forest, which could be conditioned by temperature and precipitation [35].

Assessing LULC changes in forest ecosystems is an important tool that helps to multitemporal changes and manage forests with high biodiversity [59]. In the period of analysis, an increase in urban areas was reported, which could be related to urbanization and population growth that demands more and more housing and crop planting [60, 61]. As well as the increase in bare land areas and El Niño phenomenon that impact terrestrial ecosystems and species habitat [62, 63]. This study also reports the reduction of agricultural area, which may be related to the occurrence of ENSO in 2017 that favored agriculture with abundant rainfall and reduced poverty in rural communities by 5% in this ecosystem [64], however, this phenomenon occurs between 3 to 8 years, which conditions agriculture in these areas [39]. The dense dry forest decreased and the open dry forest increased. This reduction may be related to the establishment of new plots for agriculture, urban growth and selective logging [38].

The creation of PA is considered an agent to mitigate deforestation problems and prevent the loss of forest species [65, 66]. At the PA level in the dry forest, it was reported that 92.78% of the conserved area remained unaltered with respect to its natural cover. However, 2.45% of its area lost its forest cover. It is evident that PAs experience a deforestation process both inside and outside their buffer zones [67, 68], with logging being one of the causes of forest loss [69]. Likewise, it has been shown that PA peripheral areas and intangible areas are exposed to deforestation problems [70] due to anthropogenic activities and cattle ranching [67, 71].

The highest degree of intensity is mainly found in the urban and agricultural classes. Cui et al. [58] consider that high values are related to a high degree of anthropogenic impacts, high levels of LULC with flat slopes. On the other hand, the largest area that presented a low degree of land use were the soil classes with or without vegetation, water bodies and forests for being less impacted by human activities and for being on high slopes [55].

The use of the GEE platform offers the ability to process large volumes of data and can be applied for LULC change analysis of large surface areas and crop mapping [25]. A disadvantage when taking images is the problems of cloudiness and the effect of sea swell that can complicate LULC mapping in certain areas, for which atmospheric correction through different algorithms is necessary [72]. In addition, the creation of mosaics with a wider range of dates and complemented with other images such as Landsat, PlanetScope and Sentinel-1A. Special and temporal resolution are other important aspects to be taken into account in LULC studies, the higher the spatial resolution, the greater the LULC detail. While, the temporal resolution will allow obtaining a greater number of images of the same place, which will translate into greater computational power for processing.

The study provides important information as a baseline for monitoring and the formulation of recovery and conservation projects by the competent institutions. The maps present the areas where forest loss was recorded. However, future studies could improve their pressure by using more advanced classification techniques such as image segmentation and deep learning and the use of high-resolution satellite images such as PlanetScope [51]. In addition, future studies need to analyze a larger number of LULC classes and longer time periods to generate multi-temporal historical information [73].

5. CONCLUSIONS

In this research we analysed LULC changes in the dry forest using cloud computing. The LULC maps obtained reported pressures higher than 85%. In the study area, there was a reduction of cultivated land and dense dry forest, while urban areas, dense soils and open dry forest increased significantly. From the perspective of changes in the LULC, it was found that agricultural areas were mainly changed into bare soils and urban areas. On the other hand, natural protected areas showed forest loss, indicating impacts from population and climate change.

The results of this study report the changes of LULC in the dry forest of Peru. This information can be used as a baseline for identifying deforested areas and developing actions for their recovery and conservation by decision makers. In the future, it is important to conduct research that integrates longer time periods and their future prediction using SR techniques, as well as social, economic and environmental aspects to improve the management and conservation of this important dry forest ecosystem.

ACKNOWLEDGMENT

We would like to thank the Dirección de Desarrollo Tecnológico Agropecuario – DDTA of the Instituto Nacional de Innovación Agraria – INIA. This research was conducted and financed mainly by CUI Project No 2253484 "Creación de un Servicio de Laboratorio de Agrostología de la Universidad Nacional Toribio Rodríguez de Mendoza" that was financed by Sistema Nacional de Inversión Pública (SNIP) of the Ministry of Economy and Finance (MEF) of Peru. Also, was supported by the Vice-Rectorate of Research of the Universidad Nacional Toribio Rodríguez de Mendoza de Amazonas - UNTRM.

REFERENCES

[1] Lehmann, C.E.R., Archibald, S.A., Hoffmann, W.A., Bond, W.J. (2011). Deciphering the distribution of the savanna biome. New Phytologist, 191(1): 197-209. https://doi.org/10.1111/j.1469-8137.2011.03689.x

[2] Miles, L., Newton, A.C., DeFries, R.S., Ravilious, C., May, I., Blyth, S., Kapos, V., Gordon, J.E. (2006). A global overview of the conservation status of tropical dry forests. Journal of Biogeography, 33(3): 491-505. https://doi.org/10.1111/j.1365-2699.2005.01424.x

[3] Sullivan, M.J.P., Talbot, J., Lewis, et al. (2017). Diversity and carbon storage across the tropical forest biome. Scientific Reports, 7: 1-12. https://doi.org/10.1038/srep39102

[4] Pötzschner, F., Baumann, M., Gasparri, N.I., Conti, G., Loto, D., Piquer-Rodríguez, M., Kuemmerle, T. (2022). Ecoregion-wide, multi-sensor biomass mapping highlights a major underestimation of dry forests carbon stocks. Remote Sensing of Environment, 269: 1-10. https://doi.org/10.1016/j.rse.2021.112849

[5] An, Y., Zhao, W., Li, C., Sofia Santos Ferreira, C. (2022). temporal changes on soil conservation services in large basins across the world. Catena, 209: 105793. https://doi.org/10.1016/j.catena.2021.105793

[6] Keys, P.W., Wang-Erlandsson, L., Gordon, L.J. (2016). Revealing invisible water: Moisture recycling as an ecosystem service. PLoS One, 11: 1-16. https://doi.org/10.1371/journal.pone.0151993

[7] Stefanidis, S., Alexandridis, V., Ghosal, K. (2022). Assessment of water-induced soil erosion as a threat to natura 2000 protected areas in Crete Island, Greece. Sustainability, 14: 1-22. https://doi.org/10.3390/su14052738

[8] Powers, J.S., Feng, X., Sanchez-Azofeifa, A., Medvigy, D. (2018). Focus on tropical dry forest ecosystems and ecosystem services in the face of global change. Environmental Research Letters, 13. https://doi.org/10.1088/1748-9326/aadeec

[9] Reyes-Palomeque, G., Dupuy, J.M., Portillo-Quintero, C.A., Andrade, J.L., Tun-Dzul, F.J., Hernández-Stefanoni, J.L. (2021). Mapping forest age and

characterizing vegetation structure and species composition in tropical dry forests. Ecological Indicators, 120. https://doi.org/10.1016/j.ecolind.2020.106955
[10] Singh, C., Karan, S.K., Sardar, P., Samadder, S.R. (2022). Remote sensing-based biomass estimation of dry deciduous tropical forest using machine learning and ensemble analysis. Journal of Environmental Management, 308: 114639. https://doi.org/10.1016/j.jenvman.2022.114639
[11] Qarallah, B., Al-Ajlouni, M., Al-Awasi, A., Alkarmy, M., Al-Qudah, E., Naser, A.B., Al-Assaf, A., Gevaert, C.M., Al Asmar, Y., Belgiu, M., Othman, Y.A. (2021). Evaluating post-fire recovery of latroon dry forest using landsat ETM+, unmanned aerial vehicle and field survey data. Journal of Arid Environments, 193: 104587. https://doi.org/10.1016/j.jaridenv.2021.104587
[12] Winkler, K., Fuchs, R., Rounsevell, M., Herold, M. (2021). Global land use changes are four times greater than previously estimated. Nature Communications, 12: 1-10. https://doi.org/10.1038/s41467-021-22702-2
[13] Mendoza-Ponce, A., Corona-Núñez, R., Kraxner, F., Leduc, S., Patrizio, P. (2018). Identifying effects of land use cover changes and climate change on terrestrial ecosystems and carbon stocks in Mexico. Global Environmental Change, 53: 12-23. https://doi.org/10.1016/j.gloenvcha.2018.08.004
[14] Corona-Núñez, R.O., Mendoza-Ponce, A.V., Campo, J. (2021). Assessment of above-ground biomass and carbon loss from a tropical dry forest in Mexico. Journal of Environmental Management, 282. https://doi.org/10.1016/j.jenvman.2021.111973
[15] Foley, J.A., DeFries, R., Asner, et al. (2005). Global consequences of land use. Science, 309: 570-574. https://www.science.org/doi/10.1126/science.1111772.
[16] Netzer, M.S., Sidman, G., Pearson, T.R.H., Walker, S.M., Srinivasan, R. (2019). Combining global remote sensing products with hydrological modeling to measure the impact of tropical forest loss on water-based ecosystem services. Forests, 10: 1-20. https://doi.org/10.3390/f10050413
[17] Zhu, E., Deng, J., Zhou, M., Gan, M., Jiang, R., Wang, K., Shahtahmassebi, A.R. (2019). Carbon emissions induced by land-use and land-cover change from 1970 to 2010 in Zhejiang, China. Science of the Total Environment, 646: 930-939. https://doi.org/10.1016/j.scitotenv.2018.07.317
[18] Rojas, N.B., Barboza, E., Maicelo, J.L., Oliva, S.M., Salas, R. (2019). Deforestación en la Amazonía Peruana: Índices de cambios de cobertura y uso del suelo basado en SIG. Boletín de la Asociación de Geógrafos Españoles, 81: 1-34. https://doi.org/10.21138/bage.2538a
[19] Iqbal, M.F., Khan, I.A. (2014). Spatiotemporal land use land cover change analysis and erosion risk mapping of Azad Jammu and Kashmir, Pakistan. Egyptian Journal of Remote Sensing and Space Science, 17: 209-229. https://doi.org/10.1016/j.ejrs.2014.09.004
[20] Achmad, A., Ramli, I., Sugiarto, S., Irzaidi, I., Izzaty, A. (2024). Assessing and forecasting carbon stock variations in response to land use and land cover changes in central Aceh, Indonesia. International Journal of Design & Nature and Ecodynamics, 19: 465-475. https://www.iieta.org/journals/ijdne/paper/10.18280/ijdne.190212.
[21] Yahya, N., Bekele, T., Gardi, O., Blaser, J. (2020). Forest cover dynamics and its drivers of the arba gugu forest in the eastern highlands of Ethiopia during 1986 - 2015. Remote Sensing Applications: Society and Environment, 20: 100378. https://doi.org/10.1016/j.rsase.2020.100378
[22] Edewede, D., Onojiede, E., Peace, N. (2019). Effect of urban centre growth on vegetation cover: A case study of Ebony State, South-Eastern, Nigeria. Environmental Earth Sciences Research Journal, 6: 51-58. https://www.iieta.org/journals/eesrj/paper/10.18280/eesrj.060201.
[23] de Luque-Villa, M., Acosta-Santos, C., Vargas-Cediel, A., Robledo-Buitrago, D. (2020). Noise impact assessment using corine land cover methodology: A case study in Funza, Colombia. International Journal of Sustainable Development and Planning, 15: 857-863. https://www.iieta.org/journals/ijsdp/paper/10.18280/ijsdp.150609
[24] Andrade, J., Cunha, J., Silva, J., Rufino, I., Galvão, C. (2021). Evaluating single and multi-date landsat classifications of land-cover in a seasonally dry tropical forest. Remote Sensing Applications: Society and Environment, 22: 100515. https://doi.org/10.1016/j.rsase.2021.100515
[25] Tamiminia, H., Salehi, B., Mahdianpari, M., Quackenbush, L., Adeli, S., Brisco, B. (2020). Google Earth Engine for geo-big data applications: A meta-analysis and systematic review. ISPRS Journal of Photogrammetry and Remote Sensing, 164: 152-170. https://doi.org/10.1016/j.isprsjprs.2020.04.001
[26] Man, C.D., Nguyen, T.T., Bui, H.Q., Lasko, K., Nguyen, T.N.T. (2018). Improvement of land-cover classification over frequently cloud-covered areas using landsat 8 time-series composites and an ensemble of supervised classifiers. International Journal of Remote Sensing, 39: 1243-1255. https://doi.org/10.1080/01431161.2017.1399477
[27] Wulder, M.A., White, J.C., Loveland, T.R., Woodcock, C.E., Belward, A.S., Cohen, W.B., Fosnight, E.A., Shaw, J., Masek, J.G., Roy, D.P. (2016). The global landsat archive: status, consolidation, and direction. Remote Sensing of Environment, 185: 271-283. https://doi.org/10.1016/j.rse.2015.11.032
[28] Teluguntla, P., Thenkabail, P., Oliphant, A., Xiong, J., Gumma, M.K., Congalton, R.G., Yadav, K., Huete, A. (2018). A 30-m landsat-derived cropland extent product of australia and china using random forest machine learning algorithm on google earth engine cloud computing platform. ISPRS Journal of Photogrammetry and Remote Sensing, 144: 325-340. https://doi.org/10.1016/j.isprsjprs.2018.07.017
[29] Belgiu, M., Drăgu, L. (2016). Random forest in remote sensing: A review of applications and future directions. ISPRS Journal of Photogrammetry and Remote Sensing, 114: 24-31. https://doi.org/10.1016/j.isprsjprs.2016.01.011
[30] Melo, M.V.N. de, Oliveira, M.E.G. de, Almeida, G.L.P. de, Gomes, N.F., Montalvo Morales, K.R., Santana, T.C., Silva, P.C., Moraes, A.S., Pandorfi, H., Silva, M.V. (2022). Spatiotemporal characterization of land cover and degradation in the agreste region of pernambuco, brazil, using cloud geoprocessing on Google Earth Engine. Remote Sensing Applications: Society and Environment, 26: 00756.

https://doi.org/10.1016/j.rsase.2022.100756
[31] Huang, H., Chen, Y., Clinton, N., Wang, J., Wang, X., Liu, C., Gong, P., Yang, J., Bai, Y., Zheng, Y., Zhu, Z. (2017). Mapping major land cover dynamics in beijing using all landsat images in Google Earth Engine. Remote Sensing of Environment, 202: 166-176. https://doi.org/10.1016/j.rse.2017.02.021
[32] Na, X., Zhang, S., Li, X., Yu, H., Liu, C. (2010). Improved land cover mapping using random forests combined with landsat thematic mapper imagery and ancillary geographic data. Photogrammetric Engineering and Remote Sensing, 76: 833-840. https://doi.org/10.14358/pers.76.7.833
[33] Gonzáles, P., Neri, L. (2015). El ecoturismo como alternativa sostenible para proteger el bosque seco tropical peruano: El caso de proyecto hualtaco, tumbes. PASOS Revista de Turismo y Patrimonio Cultural, 13: 1437-1449. https://www.redalyc.org/articulo.oa?id=88143407012.
[34] Mercado, W., Rimac, D. (2019). Comercialización de miel de abeja del bosque seco, distrito de Motupe, Lambayeque, Perú. Natura@economía, 4: 24. https://doi.org/10.21704/ne.v4i1.1358
[35] Zorogastúa, P., Quiroz, R., Garatuza, J. (2011). Evaluación de cambios en la cobertura y uso de la tierra con imágenes de satélite en Piura - Perú. Ecología Aplicada, 10: 13-22. http://www.scielo.org.pe/scielo.php?pid=S1726-22162011000100002&script=sci_abstract.
[36] Aldana, C., Revilla, M., Gonzales, J., Saavedra, Y., Moncada, W., Maicelo, J. (2020). Relación de firmas espectrales para la identificación de bosque seco en imágenes de satélite Sentinel 2, cuenca baja del río Chira, región Piura. Revista de Teledetección, 147. https://doi.org/10.4995/raet.2020.14110
[37] Pennington, R.T., Prado, D.E., Pendry, C.A., Garden, R.B. (2001). Neotropical seasonally dry forests and quaternary vegetation changes. Journal of Biogeography, 27: 261-273. https://doi.org/10.1046/j.1365-2699.2000.00397.x
[38] MINAM. (2018). Línea de base de los bosques secos de la costa norte del Perú al 2018. Ministerio del Ambiente, Lima, Perú. Available online: http://www.bosques.gob.pe/archivo/Apuntes-del-bosque-4.pdf.
[39] Rodríguez, A., Álvarez, R. (2005). Uso múltiple del bosque seco del norte del Perú: análisis del ingreso y autoconsumo. Zonas Áridas, 8921: 131-148.
[40] Ruíz, L., Quijandría, G., Otárola, E., Rios, S., Álvarez, J., Núñez, F. (2019). Mapa nacional de ecosistemas del Perú: memoria descriptiva. Ministerio del Ambiente, Lima, Perú. Available online: http://www.bosques.gob.pe/archivo/Apuntes-del-bosque-4.pdf.
[41] Moro, M.F., Silva, I.A., De Araújo, F.S., Lughadha, E.N., Meagher, T.R., Martins, F.R. (2015). The role of edaphic environment and climate in structuring phylogenetic pattern in seasonally dry tropical plant communities. PLoS One, 10: 1-18. https://doi.org/10.1371/journal.pone.0119166
[42] Chuvieco, E. (2020). Fundamentals of satellite remote sensing: An environmental approach. CRC Press, Boca Raton.
[43] Parente, L., Ferreira, L. (2018). Assessing the spatial and occupation dynamics of the brazilian pasturelands based on the automated classification of modis images from 2000 to 2016. Remote Sensing, 10: 606. https://doi.org/10.3390/rs10040606
[44] Gorelick, N., Hancher, M., Dixon, M., Ilyushchenko, S., Thau, D., Moore, R. (2017). Google earth engine: planetary-scale geospatial analysis for everyone. Remote Sensing of Environment, 202: 18-27. https://doi.org/10.1016/j.rse.2017.06.031
[45] Breiman, L. (2001). Random Forests. Machine Learning, 45: 5-32. https://doi.org/10.1023/A:1010933404324
[46] Hosseiny, B., Abdi, A.M., Jamali, S. (2022). Urban land use and land cover classification with interpretable machine learning - A case study using Sentinel-2 and auxiliary data. Remote Sensing Applications: Society and Environment, 28. https://doi.org/10.1016/j.rsase.2022.100843
[47] Traganos, D., Reinartz, P. (2018). Mapping mediterranean seagrasses with Sentinel-2 imagery. Marine Pollution Bulletin, 134: 197-209. https://doi.org/10.1016/j.marpolbul.2017.06.075
[48] Tsai, Y.H., Stow, D., Chen, H.L., Lewison, R., An, L., Shi, L. (2018). Mapping Vegetation and Land Use Types in Fanjingshan National Nature Reserve Using Google Earth Engine. Remote Sensing, 10(6): 927. https://doi.org/10.3390/rs10060927
[49] Foody, G.M. (1992). On the compensation for chance agreement in image classification accuracy assessment. Photogrammetric Engineering and Remote Sensing, 58: 1459-1460. https://www.asprs.org/wp-content/uploads/pers/1992journal/oct/1992_oct_1459-1460.pdf.
[50] Cochran, W.G. (1997). Sampling Techniques. John Wiley, Hoboken.
[51] Acharki, S. (2022). PlanetScope contributions compared to Sentinel-2, and Landsat-8 for LULC mapping. Remote Sensing Applications: Society and Environment, 27: 100774. https://doi.org/10.1016/j.rsase.2022.100774
[52] Padilla, M., Stehman, S.V., Chuvieco, E. (2014). Validation of the 2008 MODIS-MCD45 global burned area product using stratified random sampling. Remote Sensing of Environment, 144: 187-196. https://doi.org/10.1016/j.rse.2014.01.008
[53] Pontius, R.G., Shusas, E., McEachern, M. (2004). Detecting important categorical land changes while accounting for persistence. Agriculture, Ecosystems & Environment, 101: 251-268. https://doi.org/10.1016/j.agee.2003.09.008
[54] FAO. (1996). Forest Resources Assessment 1990. Survey of Tropical Forest Cover and Study of Change Processes. Rome, Italy. https://www.fao.org/4/w0015e/w0015e00.htm
[55] Zhang, S., Guan, Z., Liu, Y., Zheng, F. (2022). Land use/cover change and its relationship with regional development in Xixian New Area, China. Sustainability, 14: 6889. https://doi.org/10.3390/su14116889
[56] Zhuang, D., Liu, J. (1997). Modeling of regional differentiation of land-use degree in China. Chinese Geographical Science, 7: 302-309. https://link.springer.com/article/10.1007/s11769-997-0002-4

[57] FAO. (2007). Situación de los Bosques del Mundo. Rome, Italy. https://www.fao.org/4/a0773s/a0773s00.htm.

[58] Cui, J., Zhu, M., Liang, Y., Qin, G., Li, J., Liu, Y. (2022). Land use/land cover change and their driving factors in the yellow river basin of shandong province based on Google Earth Engine from 2000 to 2020. ISPRS International Journal of Geo-Information, 11(3): 163. https://doi.org/10.3390/ijgi11030163

[59] Heredia-R, M., Torres, B., Cabrera-Torres, F., Torres, E., Díaz-Ambrona, C.G.H., Pappalardo, S.E. (2021). land use and land cover changes in the diversity and life zone for uncontacted indigenous people: deforestation hotspots in the Yasuní Biosphere Reserve, Ecuadorian Amazon. Forests, 12(11): 1539. https://doi.org/10.3390/f12111539

[60] Xie, H. (2017). Towards sustainable land use in china: A collection of empirical studies. Sustainability, 9(11): 2129. https://doi.org/10.3390/su9112129

[61] Zuo, Q., Li, X., Hao, L., Hao, M. (2020). Spatiotemporal evolution of land-use and ecosystem services valuation in the belt and road initiative. Sustainability, 12: 6583. https://doi.org/10.3390/su12166583

[62] Bertrand, R., Lenoir, J., Piedallu, C., Dillon, G.R., De Ruffray, P., Vidal, C., Pierrat, J.C., Gégout, J.C. (2011). Changes in plant community composition lag behind climate warming in lowland forests. Nature, 479: 517-520. https://doi.org/10.1038/nature10548

[63] Khanal, S., Timilsina, R., Behroozian, M., Peterson, A.T., Poudel, M., Alwar, M.S.S., Wijewickrama, T., Osorio-Olvera, L. (2022). Potential impact of climate change on the distribution and conservation status of pterocarpus marsupium, a near threatened South Asian medicinal tree species. Ecological Informatics, 70: 101722. https://doi.org/10.1016/j.ecoinf.2022.101722

[64] Pécastaing, N., Chávez, C. (2020). The impact of el niño phenomenon on dry forest-dependent communities' welfare in the Northern Coast of Peru. Ecological Economics, 178: 106820. https://doi.org/10.1016/j.ecolecon.2020.106820

[65] Rosa, I.M.D., Purves, D., Souza, C., Ewers, R.M. (2013). Predictive modelling of contagious deforestation in the Brazilian Amazon. PLoS One, 8: e77231. https://doi.org/10.1371/journal.pone.0077231

[66] Steege, H. Ter, Pitman, N.C.A., Killeen, et al. (2015). Estimating the global conservation status of more than 15,000 amazonian tree species. Science Advances, 1: 9-11. https://www.science.org/doi/10.1126/sciadv.1500936.

[67] Cotrina, A., Bandopadhyay, S., Rojas, N.B., Banerjee, P., Torres, C., Oliva, M. (2021). Peruvian Amazon disappearing: Transformation of protected areas during the last two decades (2001-2019) and potential future deforestation modelling using cloud computing and MaxEnt Approach. Journal of Nature Conservation, 64: 126081. https://doi.org/10.1016/j.jnc.2021.126081

[68] Paiva, P.F.P.R., de Lourdes, M., da Silva, O.M., de Nazaré, M., Braga, T.G.M., de Andrade, M.M.N., dos Santos, P.C., da Rocha, E.S., de Freitas, T.P.M., da Silva, et al. (2020). Deforestation in Protect areas in the Amazon: A threat to biodiversity. Biodiversity and Conservation, 29: 19-38. https://doi.org/10.1007/s10531-019-01867-9

[69] Cotrina, A., Barboza, E., Rojas Briceño, N.B., Oliva, M., Torres, C., Amasifuen, C.A., Bandopadhyay, S. (2020). Distribution models of timber species for forest conservation and restoration in the Andean-Amazonian Landscape, North of Peru. Sustainability, 12(19): 7945. https://doi.org/10.3390/su12197945

[70] Bonilla-Bedoya, S., Estrella-Bastidas, A., Molina, J.R., Herrera, M.Á. (2018). Socioecological system and potential deforestation in Western Amazon forest landscapes. Science of the Total Environment, 644: 1044-1055. https://doi.org/10.1016/j.scitotenv.2018.07.028

[71] Geist, H.J., Lambin, E.F. (2002). Proximate causes and underlying driving forces of tropical deforestation. BioScience, 52(2): 143-150. https://doi.org/10.1641/0006-3568(2002)052[0143:PCAUDF]2.0.CO;2

[72] Samsammurphy. (2023). Cloud Masking with Sentinel 2. GitHub Repository. https://github.com/samsammurphy/cloud-masking-sentinel2/blob/master/cloud-masking-sentinel2.ipynb.

[73] Liu, S., Li, X., Chen, D., Duan, Y., Ji, H., Zhang, L., Chai, Q., Hu, X. (2020). Understanding land use/land cover dynamics and impacts of human activities in the mekong delta over the last 40 years. Global Ecology and Conservation, 22: e00991. https://doi.org/10.1016/j.gecco.2020.e00991

NOMENCLATURE

AL	Agricultural land
BL	Bare land
DDF	Dense dry forest
ENSO	El Niño-Southern Oscillation
EVI	Enhanced Vegetation Index
GEE	Google Earth Engine
LULC	Land Use and Land Cover
ML	Machine learning
NDVI	Normalized Difference Vegetation Index
NDWI	Normalized Difference Water Index
ODF	Open dry forest
OA	Overall accuracy
PA	Producer's accuracy
RF	Random forest
S2	Sentinel-2
SAVI	Soil Adjusted Vegetation Index
UA	Urban area
UP	User's accuracy
WB	Water body

APPENDIX

Table A1. Matrix of cross-tabulation, rate of change and indices of change for LULC in the dry forest Peru (area in km^2 and %)

2017	2021						Total 2017 (km^2)	Exchange Rate (s)	Loss	Total Change	Net Change	Exchange
	UA	**AL**	**LW**	**WB**	**DDF**	**ODF**		**Percentage (%)**				
UA	11.85	0.62	4.40	0.00	0.04	0.92	17.83	17.75	33.56	159.38	92.26	67.12
AL	4.18	1,104.23	824.81	2.19	254.17	1,191.46	3,381.04	-10.20	67.34	99.71	34.97	64.74
LW	15.56	242.47	9,012.91	4.72	16.24	1,198.58	10,490.49	1.56	14.08	34.56	6.39	28.17
WB	0.04	1.06	6.44	6.61	1.95	1.35	17.44	-3.33	62.09	111.53	12.65	98.88
DDF	0.22	224.86	68.77	0.34	6,598.46	1267.87	8,160.51	-0.16	19.14	37.64	0.65	36.99
ODF	2.45	625.37	1,243.34	1.37	1,236.80	11,272.84	14,382.16	0.94	21.62	47.07	3.83	43.24
Total 2021 (km^2)	34.29	2,198.60	11,160.67	15.23	8,107.66	14,933.03	**36,449.48**					
Gain (%)	**125.82**	**32.37**	**20.47**	**49.44**	**18.49**	**25.45**						

Table A2. Statistical validation of LULC in 2017

Classification	**Reference**						**Total**	**User's** Accuracy (%)	**Commission Error** (%)
	UA	**AL**	**LW**	**WB**	**DDF**	**ODF**			
UA	22	0	3	0	0	0	25	0.88	0.12
AL	1	31	6	1	3	8	50	0.62	0.38
LW	0	1	114	0	0	5	120	0.95	0.05
WB	0	0	4	14	3	0	21	0.67	0.33
DDF	0	0	3	0	95	2	100	0.95	0.05
ODF	0	0	12	0	0	128	140	0.91	0.09
Total	23	32	142	15	101	143	456		
Producer's Accuracy (%)	0.96	0.97	0.80	0.93	0.94	0.90			
Omission Error (%)	0.04	0.03	0.20	0.07	0.06	0.10			

Table A3. Statistical validation of LULC in 2021

Classification	**Reference**						**Total**	**User's** Accuracy (%)	**Commission Error** (%)
	UA	**AL**	**LW**	**WB**	**DDF**	**ODF**			
UA	21	1	0	0	0	3	25	0.84	0.16
AL	0	40	2	0	2	6	50	0.80	0.20
LW	0	1	118	0	0	1	120	0.98	0.02
WB	0	0	3	18	0	0	21	0.86	0.14
DDF	0	0	2	0	98	0	100	0.98	0.02
ODF	0	0	17	0	13	110	140	0.79	0.21
Total	21	42	142	18	113	120	456		
Producer's Accuracy (%)	1.00	0.95	0.83	1.00	0.87	0.92			
Omission Error (%)	0.00	0.05	0.17	0.00	0.13	0.08			